Materials Research. 2023; 26:e20230172
DOI: https://doi.org/10.1590/1980-5373-MR-2023-0172

Forming Model Optimization and Microstructural Analysis of Medical Biological Porous Scaffolds Fabricated by Selective Laser Melting (SLM)

Shubo Xu[a]*, Hanlin Wang[a], Xianmeng Xue[a], Yuefei Pan[a], Baoxuan Liu[a], Xiaoyu Ju[a]

[a]Shandong Jianzhu University, School of Materials Science and Engineering, 250101, Jinan, P. R. China.

Received: March 19, 2023; Revised: May 21, 2023; Accepted: June 05, 2023

Optimally designed bone implants with a suitable porous structure have similar mechanical properties to bone tissue and at the same time have good biocompatible and excellent bioactivity. The preparation of medical biological porous scaffolds by metal 3D printing technology is one of the most promising and attractive biomedical applications. The traditional regular porous and self-growing porous scaffolds were established by using CAD and C4D software, and the different scaffolds of three-dimensional models in similar porosity was obtained. A three-dimensional model of a scaffold with a porous structure was designed, and the porous scaffold was prepared by selective laser melting (SLM) technique, and its microstructure and mechanical properties were analysed. Under the similar porosity, the average hardness of the surface of the self-growing structure porous scaffold reached 236.5HV, and the stress at 5% compressive strain after heat treatment was close to 75 MPa. The original surface of the 316L porous scaffold made by SLM has the potential to effectively promote the differentiation of MG63 cells into osteoblasts. At the same time, the surface morphology and structure of the self-growth scaffold are similar to human cancellous bone, which is conducive to cell attachment and growth, so it is more suitable for repairing diseased parts of human bones.

Keywords: *Selective laser melting (SLM), porous biomaterial, self-growing porous scaffolds, mechanical properties.*

1. Introduction

Since the 1970s, porous scaffolds have gradually been widely used in medical biological bones. Now, selective laser melting (SLM) technology can build precise and complex scaffolds by layer-by-layer printing[1,2], which effectively controls the porosity. The suitable pore size, porosity, void distribution, and pore structure of the scaffold can well solve problems such as stress shielding caused by mismatch of elastic modulus during bone repair. In recent years, 3D printing technology has become a hot research direction in the field of advanced manufacturing technology for materials and has attracted a lot of attention from academics, medical industry personnel and healthcare workers. Due to various bone diseases and bone loss caused by the infection and destruction of bone tissue and abnormal bone development, and the strength of the porous implants is different at different ages and diseased parts. Therefore, it is difficult to match the stress of the porous implant with the surrounding bone tissue. At present, this is a big problem that bothers researchers, so in-depth research on porous implants has become a trend.

Metal 3d printed implants are widely used in the field of orthopaedics, especially for artificial joints. Currently, common metal materials used in clinical medicine for bio-scaffold materials include: 316/316L stainless steel, Ti6Al4V, and cobalt-chromium alloy. 316L stainless steel is one of the medical metal materials currently used internationally, which has mechanical properties close to human bone tissue and has the advantages of good biocompatibility, corrosion resistance, high strength, good processability and low cost[3-5]. As medical implants face different groups of people, the porous scaffold has different specifications, complex shapes, and numerous size specifications. Traditional manufacturing techniques have been difficult to meet market demand. The use of additive manufacturing technology is expected to be the perfect solution to these problems. Aiming at the question of whether the scaffold can be effectively transmitted and the stress of the surrounding bone tissue, many bone tissue researchers used selective laser melting (SLM) technology to prepare medical biological porous scaffolds, using a high-energy laser beam as a heat source, focusing on a layer by layer. The metal powder is melted and melted and solidified with the sintered solidified layer or substrate, and the scaffold is melted layer by layer to produce a scaffold of accurate size and complex shape[6]. This not only replaces the bone tissue in the affected area, but also overcomes the drawbacks of conventional methods of manufacturing porous bone implants that make it difficult to meet individual requirements.

After the porous scaffolds are implanted into the human body, the existence of pores can ensure the transmission of nutrients and metabolism, and effectively avoid the problems of stress concentration and shielding. At the same time, the porous scaffold facilitates cell growth, attachment, migration, and stimulation of blood vessel growth[7-9]. Eventually, the implant successfully fuses with the body. The 3D printing technology can effectively control the porosity and size and structure of the scaffolds formed. Effective structure design

*e-mail: xsb@sdjzu.edu.cn

can ensure the transmission of nutrients and metabolites and the reasonable distribution of stress, so as to obtain a biological porous scaffold and achieve the regeneration or transplantation of biologically-renewable bone[10]. In terms of the current state of research in porous scaffold modelling for medical biology, it is important to study the appropriate porosity and pore size, the scaffold geometry and the functional gradient structure of porous scaffold modelling for medical implants by SLM[11]. In this paper, the process of manufacturing bioactive metal porous scaffolds by using selective laser melting were discussed in detail, and the micromorphology and mechanical properties of scaffolds with different structures with similar porosity were analyzed.

2. Forming of Porous Scaffold by SLM

Optimally designed bone implants with a suitable porous structure have similar mechanical properties to bone tissue and at the same time have good biocompatible and excellent bioactivity. It is therefore important to study the modelling and forming of porous scaffolds. Figure 1 shows additive manufacturing materials for bone scaffolds. Figure 1a shows the SEM micrograph of 316L stainless steel powders. It can be seen that the 316L stainless steel powders has a spherical distribution and the powder diameter is uniformly distributed around 20um (see Figure 1b). For the particle size distribution of 316L stainless steel powders, it can be seen that the particle size of the powder meets the normal distribution rule. Table 1 shows the chemical compositions table of 316L stainless steel powders. Table 2 shows the parameters of the medical biological porous scaffolds fabricated by selective laser melting (SLM). Figure 2 gives the process of establishing a self-growing porous scaffold model, where the models in Figure 2a, 2b, 2c, and 2d were 30%, 50%, 85%, and 100%, respectively. The self-growing porous scaffold was constructed by C4D modelling software. The build method of porous scaffold model is grown using the natural growth method. The natural growth structure and morphology of human bone are restored to the greatest. The porous scaffold structures obtained by the modelling method of self-growing porous scaffolds are given in Figure 2 and Figure 3c.

Figure 3 is a solid model of porous implant scaffolds with different structures, of which (a) a model of a regular round porous scaffold, (b) a model of a regular square porous scaffold, and (c) a model of a self-growing porous scaffold, porous scaffolds with similar porosity (38-40%) but different structures were constructed by UG and C4D software[12,13].

Table 1. Chemical compositions of 316L stainless steel powders.

Materials	Ni	Cr	Mo	Mn
00Cr17Ni14 Mo2	12.0-16.0	16.0-18.0	2.0-3.0	0-2.0

Table 2. The parameters of the medical biological porous scaffolds fabricated by selective laser melting (SLM).

Laser power	scanning speed	scanning space	powder layer thickness
150.0 W	500.0 mm/s	0.06 mm	0.035 mm

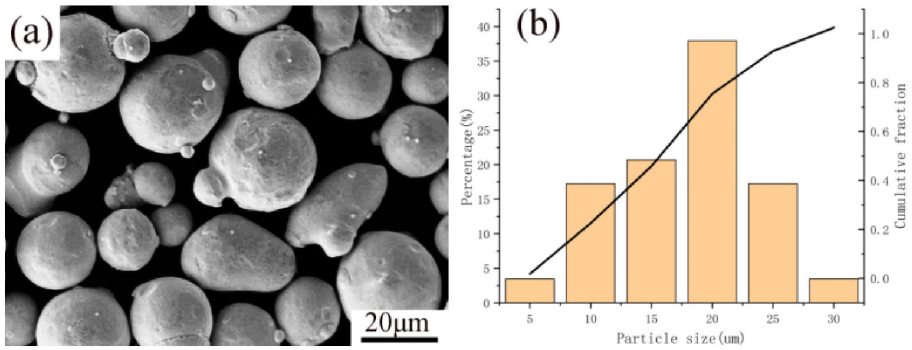

Figure 1. Additive manufacturing materials for bone scaffolds: (a) Morphology of 316L Stainless Steel Powders; (b) Particle size distribution of 316L powders.

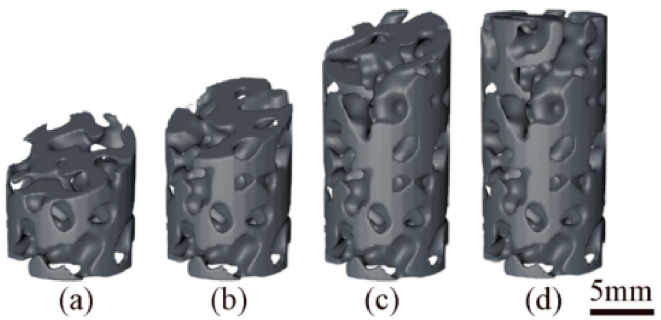

Figure 2. Establishment process of self-growing porous scaffold model.

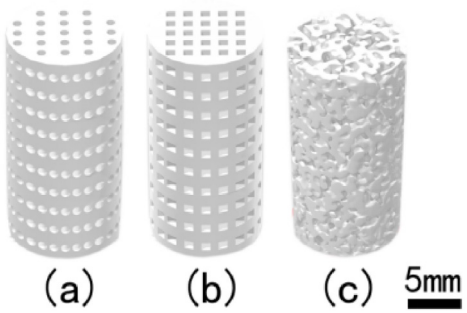

Figure 3. Additive manufacturing of bone scaffold models: (a) Model of regular square-hole porous scaffolds; (b) Model of regular square-hole round-hole scaffolds; (c) Model of self-growing porous scaffolds.

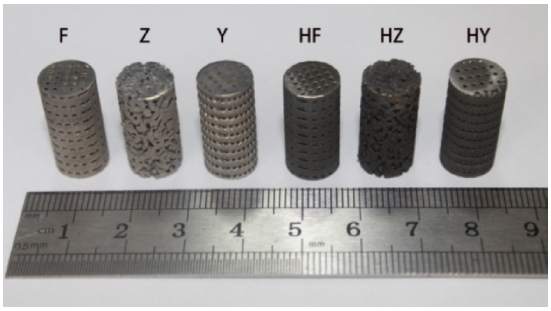

Figure 4. Different structures of 316L stainless steel porous supports fabricated by SLM:(F) regular square porous scaffold, (Z)self-growing porous scaffold, (Y) regular round porous scaffold, (HF) regular square porous scaffold after Heat Treatment, (HZ)self-growing porous scaffold after Heat Treatment, (HY) regular round porous scaffold after Heat Treatment.

Figure 4 is a 316L stainless steel porous scaffold with different structures formed by SLM, where F is the structure of a regular square porous scaffold, Z is the structure of a self-growing porous scaffold, Y is the structure of a regular round porous scaffold, HF, HZ and HY are F, Z, and Y heat-treated porous scaffolds. SLM technology was used to melting the metal powder to obtain solid porous implant scaffolds with different structures of 316L stainless steel.

Figure 5 shows optical microstruture images of medical biological porous scaffolds fabricated by selective laser melting. Figure 5a and 5b are metallographic diagrams of metallographic fiber structure formed by laser melting at 50 times and 100 times, respectively. The scanning trajectory left by SLM and sintering can be clearly seen in the sintering plane. The metallographic phase during the sintering of the layers can clearly show the welding path of the same angle in the figure, and its trajectory rotates about 60 degrees every other layer, and consists of coarse columnar dendrites, which are arranged in a good direction, and evenly distributed. SLM technology has a high solidification rate and a high gradient of solidification characteristics. The obtained structure is fine, uniform, few defects, and the microstructure is regularly arranged. Figure 5c and 5d are metallographic images of laser melting molding after heat treatment, respectively. The austenite structure could be clearly observed, but the microstructure and scanning trajectory of cell dendrites could not be clearly observed, and the boundary of the molten pool was dissolved[14].

Selective laser melting (SLM) forming technology involves powder metallurgy. After high-speed laser scanning of metal powders, metal powders will instantly melt and solidify. Therefore, during the cooling process, defects such as air bubbles and poor melting are easily generated in the formed specimens. The directly formed SLM sample has very

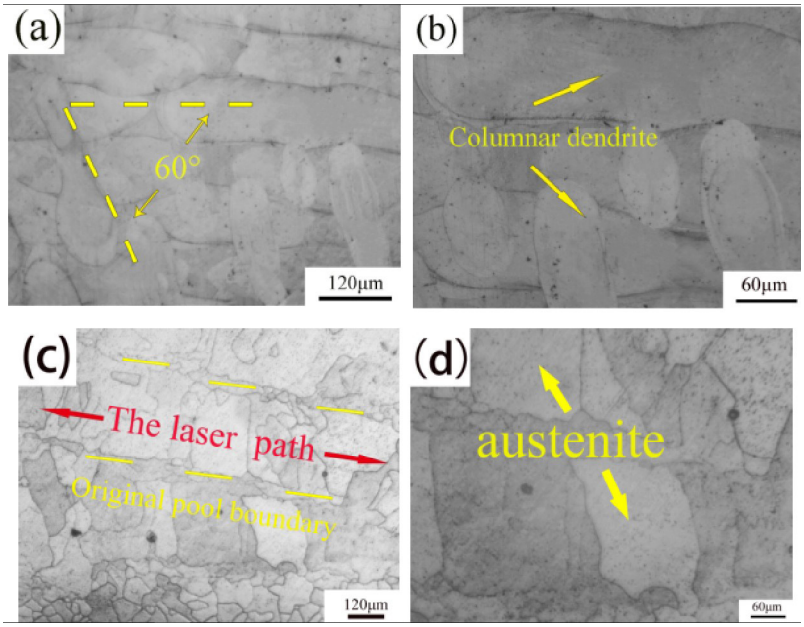

Figure 5. Optical microstruture images of medical biological porous scaffolds fabricated by selective laser melting: (a)Metallographic structure of laser melting in different directions at 50 times; (b) Metallographic structure of laser melting in different directions at 100 times; (c) Microstructure of laser melting after 100 times heat treatment; (d) Microstructure of laser melting after 200 times heat treatment.

small crystal grains, and is mainly a crescent-shaped ferrite structure with a crystal plane. The orientation difference and the grain boundary distance are large, and an unbalanced melting thermal stress is formed between each other, which causes a large amount of residual stress to be accumulated, which has a great impact on the mechanical properties of the porous scaffold.

In this paper, heat treatment is used to eliminate the residual stress, thereby improving the mechanical properties of the material. The solution and annealing heat treatment is adopted[15], as shown in the heat treatment processing route map in Figure 6. First, it is heated from 20 °C to 1050 °C. The solution treatment was carried out for 30 minutes to keep the austenite grains recrystallized, and then the temperature was lowered to 900 °C for 5 minutes, followed by annealing and aging treatment for 2 hours, followed by air cooling to room temperature.

3. Results and Analysis

3.1. Mechanical properties

Figure 7 gives Vickers hardness curve of porous scaffolds with different structures. Figure 7a shows the Vickers hardness change curve of porous supports with different structures. It can be seen from the hardness test that under the laser power of 150.0 W, the scanning rate of 500.0 mm/s, and the scanning interval of 0.06mm, the 316L stainless steel porous support is formed by SLM melting, the average hardness of traditional round-hole and square-hole porous scaffolds is 217.0 HV and 237.4 HV, respectively, but their maximum extremum is 11.3 and 48.1, respectively. However, the average hardness of self-growing porous scaffolds is 236.5 HV, and the maximum extremum is 19.9, indicating a relatively flat hardness curve.

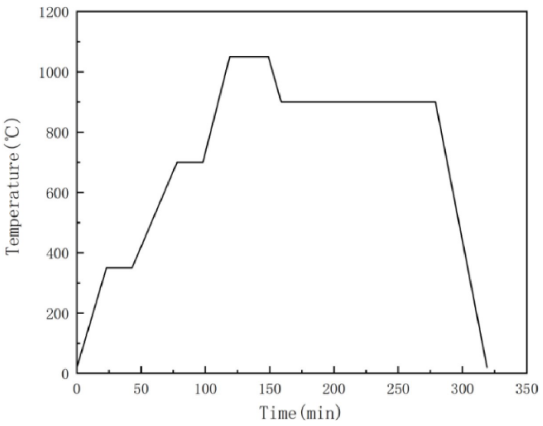

Figure 6. Heat treatment process processing route map.

At a certain volume of similar porosity, the single hole area of the traditional regular round hole scaffold is smaller than that of the square hole, resulting in a larger number of pores, which results in more pore boundaries and lower average hardness. It shows that the melting uniformity of the traditional regular small pore size porous scaffold is much lower than that of the self-growing porous scaffold under the similar porosity.

The results of heat treatment experiments show that after the solution and annealing heat treatment, the alloy elements undergo solid solution recrystallization, the grains grow, an oval austenite structure is formed, and the crystal plane orientation difference is reduced. This recrystallization promotes stress release, improves the internal structure, and reduces the δ-ferrite volume fraction, and the residual stress is significantly reduced or eliminated[16]. As shown in Figure 7b, the hardness of the Vickers hardness curve of the scaffold is significantly reduced after heat treatment of different structures. It shows that the hardness is significantly reduced. The average hardness values of HY, HF, and HZ are 181.8 HV, 199.9 HV, and 196.1 HV, respectively, compared with the average hardness of Y, F, and Z before heat treatment. They were reduced by 31.3 HV, 37, 5 HV and 40.4 HV, respectively.

The correlation between mechanical properties and geometric parameters is an important index for evaluating the controllability of porous scaffolds, and it is also the main basis for guiding design. In other words, the mechanical properties of porous scaffolds are closely related to their porosity, pore size, and scaffold structure. In addition, the heat treatment will also affect the mechanical properties of

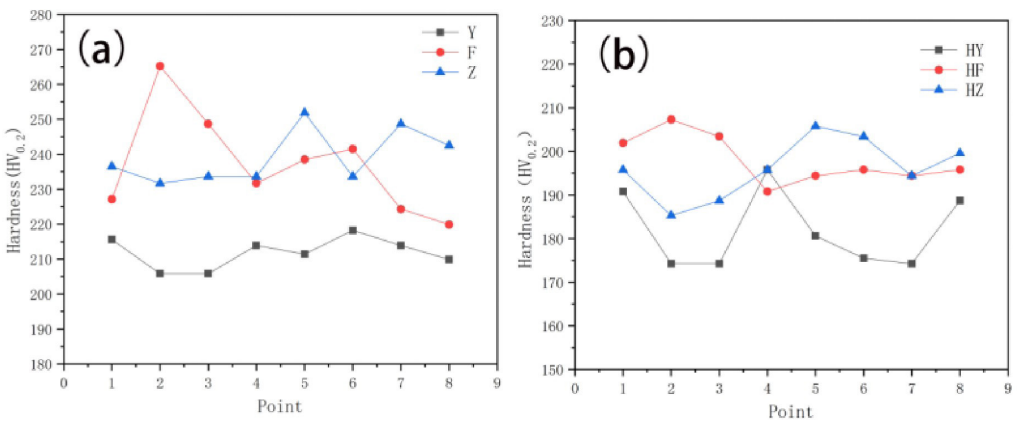

Figure 7. Vickers hardness curve of porous scaffolds with different structures: (a) Vickers hardness of different structure; (b)Vickers hardness of different structure after heat treatment.

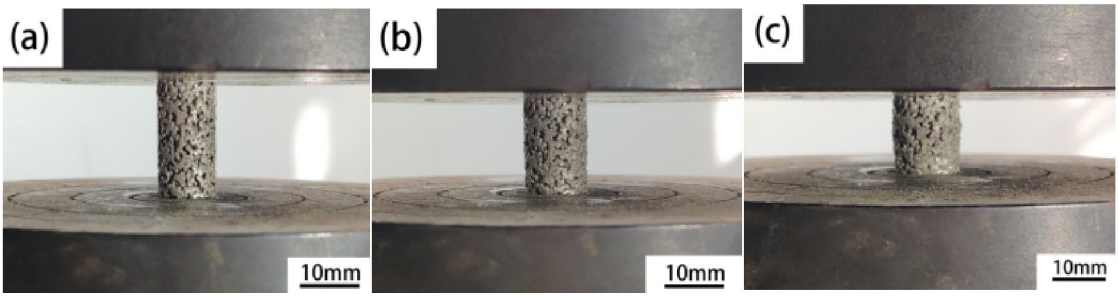

Figure 8. The compression experiments of self-growing porous scaffolds: (a) Self-growing porous scaffold compression 0%; (b) Self-growing porous scaffold compression 30%; (c) Self-growing porous scaffold compression 50%.

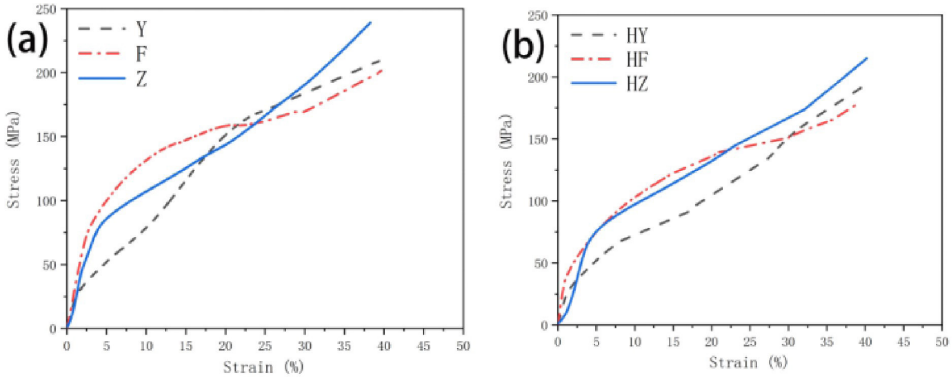

Figure 9. The stress-strain curves of porous scaffolds: (a) Stress-strain curves of regular round holes, square holes and self-growing scaffolds; (b) Stress-strain curves of regular round holes, square holes and self-growing scaffolds after heat treatment.

the SLM formed samples. The compression experiments of self-growing porous scaffolds were performed by using an electronic universal testing machine at a speed of 1mm/min,as shown in Figure 8.

Figure 9 gives the stress-strain curves of porous scaffolds. As shown in Figure 9a, the stress-strain curves of regular round holes, square holes, and self-growing scaffolds, and the stress-strain curves of regular round holes, square holes, and self-growing scaffolds after heat treatment in Figure 9b. From the stress-strain curve analysis, it can be seen that the stress value of the sample has been shaken obviously before the fracture occurred, because the local structure in the porous scaffold was crushed. When the first abrupt point appears, the pore structure inside the porous scaffold begins to deform and break; when the instability point is reached, the curve drops a distance and then continues to rise. This turning stage is when the porous scaffold is compacted and the shape changes, as a similar phenomenon occurs in Choy et al.[17].

After heat treatment, the porous scaffold materials structure is more uniform, the stress corresponding to the same strain level is reduced, the curve is smoother, and the variation range is reduced. Under natural conditions, the Young's modulus of human cancellous bone is 0.1-4.5 GPa, and the ultimate strength is 1.5-38MPa. Cortical bone has a Young's modulus of 5 to 23 GPa and an ultimate strength of 35 to 253 MPa[18,19]. The compression test results of a self-growing porous scaffold formed by SLM are in this range. From the above analysis, it can be seen that under the conditions of the same volume and the same porosity, the autogenous porous scaffold can withstand greater pressure than the conventional porous scaffold and has better stability after heat treatment.

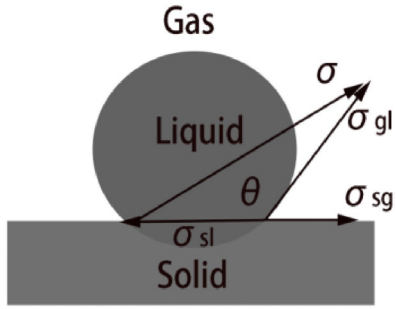

Figure 10. Schematic diagram of formation mechanism of spheroidization.

3.2. Microstructures analysis

When the metal powder is melted by laser, the shape of the molten pool mainly depends on the interfacial tension between the melt and the solid phase. Figure 10 is a schematic diagram of the spheroidization formation mechanism, and the relationship can be expressed as[20]:

$$Cos\theta = \frac{|\sigma gl|^2 + |\sigma sl|^2 - |\sigma sl - \sigma gl|^2}{2\sigma gl\sigma sl} \quad (1)$$

Among them, θ is a contact angle (also called an infiltration angle), and σ_{gl}, σ_{sg}, and σ_{sl} are the surface tension of the gas and liquid phases, the surface tension of the solid and gas phases, and the surface tension of the solid and liquid phases, respectively. The magnitude of θ angle reflects the size of the surface infiltration. With the decrease of θ angle, the surface infiltration effect in the liquid phase will be improved.

The nature of the solidification of the molten pool can be inferred by observing different microstructure characteristics. Due to the temperature change of the molten pool, the cooling rate will determine the grain size to evolve into a columnar or equiaxed structure. Figure 11 gives the forming mechanism of selective laser melting. As shown in the SEM image of powder adhesion after laser scanning in Figure 11a, near the laser scanning track, it can be noticed that the relatively low solidification rate leads to the appearance of columnar and dendritic structures[16,21]. The orientation is perpendicular to the laser beam or molten pool motion direction[22,23], which can be interpreted as the grains develop in a direction parallel to the local heat transfer and solidify in a direction perpendicular to the isotherm.

As shown in the formation mechanism of powder adhesion after laser scanning in Figure 11b, in the area near the center of the laser scanning track, small equiaxed structures (cellular structures) can be observed. These cellular structures are the powder pool in the final stage formed at a high solidification rate.At the same time, a large amount of unmelted powder adhered to the surface after laser scanning, and the molten pool actively swallowed the powder particles from the surrounding powder layer, and quickly solidified through surface tension and violent convection movement[24]. Investigations in the literature have shown[25] that in an artificial three dimensional porous scaffold, the local growth rate of osteoblasts when forming tissues is strongly influenced by the geometric characteristics of the porous channels, and the tissue surface cells can perceive the radius of curvature of the porous scaffold where they are located and react.

Figure 12 shows the SEM image of the porous structure of different porous scaffolds. Where Figure 12a shows SEM simulated cell growth images of a regular square pore porous scaffold, Figure 12b shows SEM microscopic simulated cell growth images of a regular round pore scaffold and Figure 12c shows SEM microscopic simulated cell growth images of a self-growing porous scaffold. In Figure 12a SEM micromorphology image of a regular square porous scaffold, the local curvature of the corner of a square porous channel is larger, while the curvature of the area around the corner is smaller, and the new tissue will eventually form a tubular section. Assuming that the thinnest thickness of the new tissue is 100μm, as shown in Figure 12b SEM micromorphology image of a regular round hole porous

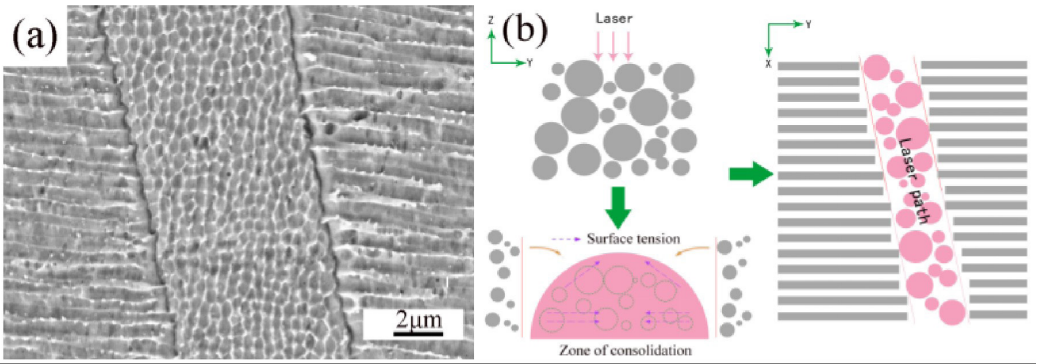

Figure 11. The forming mechanism of selective laser melting: (a) SEM image of powder adhesion after laser scanning; (b) Forming mechanism of powder adhesions after laser scanning.

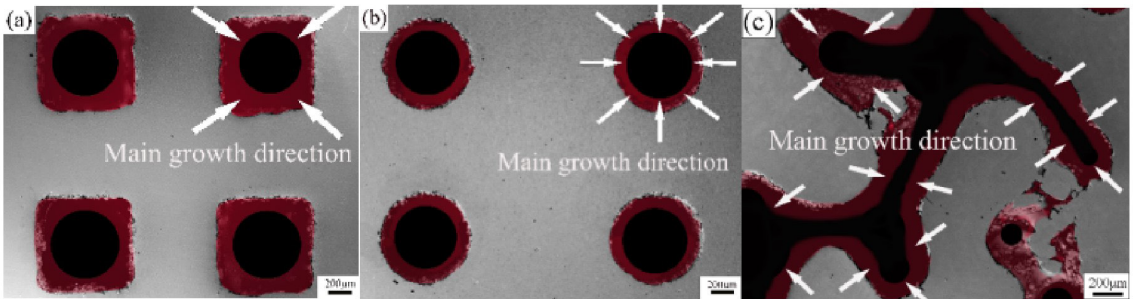

Figure 12. The SEM image of the porous structure of different porous scaffolds: (a) SEM microscopic image of regular square hole porous scaffolds; (b) SEM microscopic image of regular round hole scaffolds; (c) SEM microscopic image of self-growing porous scaffolds.

scaffold, the red area represents new tissue, which has the same curvature everywhere in the circular porous channel, so that new tissue forms evenly on the surface. In Figure 12c, SEM micromorphology image of a self-growing porous scaffold, due to the micro-scale pores, gullies and the provided physical fulcrum, the original surface of the self-growing structure porous scaffold constructed by SLM is beneficial to the early attachment, migration and proliferation of cells[26]. Compared with traditional regular round holes and regular square holes, self-growing porous scaffolds have a greater curvature driving effect, making the branch channel can be filled in a short time. Therefore, 316L self-growing porous scaffolds made by SLM have potential to effectively promote MG63 cells to differentiate into osteoblasts[27,28].

4. Conclusions

In this study, 316L porous scaffolds with regular square holes, round holes and self-growth structures with similar porosity under the same volume were constructed by using software UG and C4D. The self-growing scaffold manufactured based on the principle of random field and the method of controlling the degree of randomness can simulate the morphology and structure of cancellous bone to the greatest extent. As a typical additive manufacturing (AM) technology, the SLM process shows good processing performance in the preparation of complex porous scaffolds. Different porosity and structures have a significant impact on the mechanical properties of the scaffolds.

(1) Observation of the microstructure morphology shows that the shaped part is affected by the laser scanning path. The growth direction of the columnar dendrites is generally consistent, with good directional arrangement and uniform distribution, the angular path of the intersecting scan is 60°. Defects such as porosity and poor sintering will affect the mechanical properties of the scaffolds.

(2) Solution and annealing heat treatments can effectively improve the internal microstructure of the material of the 316L porous scaffolds prepared by SLM without significantly reducing its strength. Compared with before heat treatment, the surface hardness is reduced by 30-40 HV. The 316L porous scaffold with porosity of 38-40% has perfect mechanical properties, the surface hardness reached 196.1 HV after heat treatment. The stress of the scaffold sample reaches 5% deformation under the 75 Mpa compression test, and the mechanical properties match the human bone tissue. Under similar porosity, the hardness curve of the self-growing porous scaffold has a small change range.

(3) Observation of the surface morphology of the microstructure shows that due to the existence of micro-scale pores and gullies in the self-growing structure, the surface of the self-growing porous scaffold has a larger curvature-driven effect than the traditional regular round holes and regular square holes, cells are easier to attach, migrate and proliferate at an early stage. Therefore, the original surface of the 316L porous scaffold made by SLM has the potential to effectively promote the differentiation of MG63 cells into osteoblasts.

5. Acknowledgments

This study was supported by the Shandong Province New Old Energy Conversion Major Project (New Energy Industry 2021-03-3), Natural Science Foundation of Shandong Province, China (ZR2021ME182), National College Student Innovation and Entrepreneurship Program (S20211043001, 202210430010 and 202210430008), the Science and Technology Enterprise Innovation Program of Shandong Province, China (2022TSGC2108 and 2022TSGC2402), the High quality curriculum construction project of Shandong Jianzhu University graduate education (ALK202210).

6. References

1. Liu P, Sun SY, Xu SB, Cao MQ, Hong C, Hu JY. Effect of solid solution + double ageing on microstructure and properties in the layer by layer of the Z-Y interface of Inconel 718 alloys fabricated by SLM. Mater Res. 2018;21:e20180395.
2. Hu JY, Liu P, Sun SY, Zhao YH, Zhang YB, Huo YS. Relation between heat treatment processes and microstructural characteristics of 7075 Al alloy fabricated by SLM. Vacuum. 2020;177:109404.
3. Disegi JA, Eschbach L. Stainless steel in bone surgery. Injury. 2001;31(Suppl 4):D2-6.
4. Kannan S, Balamurugan A, Rajeswari S. Hydroxyapatite coatings on sulfuric acid treated type 316L SS and its electrochemical behaviour in Ringer's solution. Mater Lett. 2003;57(16-17):2382-9.
5. Fan X, Chen J, Zou JP, Wan Q, Zhou ZC, Ruan JM. Bone-like apatite formation on HA/316L stainless steel composite surface in simulated body fluid. Trans Nonferrous Met Soc China. 2009;19(2):347-52.
6. Peng T, Chen C. Influence of energy density on energy demand and porosity of 316L stainless steel fabricated by selective laser melting. Int J Pr Eng Man-Gt. 2018;5:47-54.
7. Guo Y, Xie K, Jiang WB, Wang L, Li GY, Zhao S et al. In vitro and in vivo study of 3D-printed porous Tantalum scaffolds for repairing bone defects. ACS Biomater Sci Eng. 2019;5(2):1123-33.
8. Lv J, Jia ZJ, Li J, Wang YE, Yang J, Xiu P et al. Electron beam melting fabrication of porous Ti6Al4V caffolds: cytocompatibility and osteogenesis. Adv Eng Mater. 2015;17(9):1391-8.
9. Cheng A, Humayun A, Cohen DJ, Boyan BD, Schwartz Z. Additively manufactured 3D porous Ti-6Al-4V constructs mimic trabecular bone structure and regulate osteoblast proliferation, differentiation and local factor production in a porosity and surface roughness dependent manner. Biofabrication. 2014;6(4):045007.
10. Fukuda A, Takemoto M, Saito T, Fujibayashi S, Neo M, Pattanayak DK et al. Osteoinduction of porous Ti implants with a channel structure fabricated by selective laser melting. Acta Biomater. 2011;7(5):2327-36.
11. Du YL, Xie HX, Mao DQ, Zhao N, Tian JF, Wang ZJ et al. Design and statistical analysis of irregular porous scaffolds for orthopedic reconstruction based on voronoi tessellation and fabricated via selective laser melting (SLM). Mater Chem Phys. 2020;239:121968-77.
12. Xu YL, Zhang DY, Hu ST, Chen RP, Gu YL, Kong XS et al. Mechanical properties tailoring of topology optimized and selective laser melting fabricated Ti6Al4V lattice structure. J Mech Behav Biomed Mater. 2019;99:225-39.
13. Mazur M, Leary M, Sun S, Vcelka M, Shidid D, Brandt M. Deformation and failure behaviour of Ti-6Al-4V lattice

structures manufactured by selective laser melting (SLM). Int J Adv Manuf Technol. 2016;84:1391-411.
14. Kong DC, Ni XQ, Dong CF, Zhang L, Man C, Yao JZ et al. Heat treatment effect on the microstructure and corrosion behavior of 316L stainless steel fabricated by selective laser melting for proton exchange membrane fuel cells. Electrochim Acta. 2018;276:293-303.
15. Kamariah MSIN, Harun WSW, Khalil NZ, Ahmad F, Ismail MH, Sharif S. Effect of heat treatment on mechanical properties and microstructure of selective laser melting 316L stainless steel. IOP Conf Series Mater Sci Eng. 2017;257(1):012021.
16. Imandoust A, Zarei-Hanzaki A, Heshmati-Manesh S, Moemeni S, Changizian P. Effects of ferrite volume fraction on the tensile deformation characteristics of dual phase twinning induced plasticity steel. Mater Des. 2013;53:99-105.
17. Choy SY, Sun CN, Leong KF, Wei J. Compressive properties of functionally graded lattice structures manufactured by selective laser melting. Mater Des. 2018;140:451.
18. Sevilla P, Aparicio C, Planell JA, Gil FJ. Comparison of the mechanical properties between tantalum and nickel–titanium foams implant materials for bone ingrowth applications. J Alloys Compd. 2007;439(1-2):67-73.
19. Xuenan GU, Zheng YF. A review on magnesium alloys as biodegradable materials. Front Mater Sci. 2010;4(2):111-5.
20. Sun YG, Zhang CJ. Microstructure evolution of TiBw/Ti composites during severe plastic deformation: spheroidization behavior. Mater Charact. 2021;171:111-5.
21. Yadollahi A, Shamsaei N, Thompson SM, Seely DW. Effects of process time interval and heat treatment on the mechanical and microstructural properties of direct laser deposited 316L stainless steel. Mater Sci Eng A. 2015;644:171-83.
22. Wang D, Song CH, Yang YQ, Bai YC. Investigation of crystal growth mechanism during selective laser melting and mechanical property characterization of 316L stainless steel parts. Mater Des. 2016;100:291-9.
23. Wu X, Sharman R, Mei J, Voice W. Direct laser fabrication and microstructure of a burn-resistant Ti alloy. Mater Des. 2002;23(3):239-47.
24. Liang HX, Yang YW, Xie DQ, Li L, Mao N, Wang CJ et al. Trabecular-like Ti-6Al-4V scaffolds for orthopedic: fabrication by selective laser melting and in vitro biocompatibility. J Mater Sci Technol. 2019;35(7):1284-97.
25. Thijs L, Verhaeghe F, Craeghs T, Van Humbeeck J, Kruth J-P. A study of the microstructural evolution during selective laser melting of Ti-6Al-4V. Acta Mater. 2010;58(9):3303-12.
26. Xue WC, Krishna BV, Bandyopadhyay A, Bose S. Processing and biocompatibility evaluation of laser processed porous titanium. Acta Biomater. 2007;3(6):1007-18.
27. Rumpler M, Woesz A, Dunlop JWC, van Dongen JT, Fratzl P. The effect of geometry on three-dimensional tissue growth. J R Soc Interface. 2008;5(27):1173-80.
28. Schwartz Z, Raz P, Zhao G, Barak Y, Tauber M, Yao H et al. Effect of micrometer-scale roughness of the surface of Ti6Al4V pedicle screws in vitro and in vivo. J Bone Joint Surg Am. 2008;90(11):2485-98.